Available online at www.sciencedirect.com
ScienceDirect
Nuclear Medicine and Biology 37 (2010) 845–851
NUCLEAR MEDICINE — AND — BIOLOGY
www.elsevier.com/locate/nucmedbio

Evaluation of a bolus/infusion protocol for ^{11}C-ABP688, a PET tracer for mGluR5

Cyrill Burger[a,*], Alexandra Deschwanden[a], Simon Ametamey[b], Anass Johayem[b], Bruno Mancosu[b], Matthias Wyss[a], Gregor Hasler[c], Alfred Buck[a]

[a]*Department of Nuclear Medicine, University Hospital, PET Center, 8091 Zürich, Switzerland*
[b]*Center for Radiopharmaceutical Science of ETH, PSI and USZ, 8091 Zürich, Switzerland*
[c]*Department of Psychiatry, University Hospital, Zürich, Switzerland*

Received 2 March 2010; accepted 12 April 2010

Abstract

^{11}C-ABP-688 is a selective tracer for the mGluR5 receptor. Its kinetics is fast and thus favourable for an equilibrium approach to determine receptor-related parameters. The purpose of this study was to test the hypothesis that the pattern of the ^{11}C-ABP688 uptake using a bolus-plus-infusion (B/I) protocol at early time points corresponds to the perfusion and at a later time point to the total distribution volume.
Methods: A bolus and a B/I study (1 h each) was performed in five healthy male volunteers. With the B/I protocol, early and late scans were normalized to gray matter, cerebellum and white matter. The same normalization was done on the maps of the total distribution volume (Vt) and K_1 which were calculated in the study with bolus only injection and the Logan method (Vt) and a two-tissue compartment model (K_1).
Results: There was an excellent correlation close to the identity line between the pattern of the late uptake in the B/I study and Vt of the bolus-only study for all three normalizations. The pattern of the early uptake in the B/I study correlated well with the K_1 maps, but only when normalized to gray matter and cerebellum, not to white matter.
Conclusion: It is demonstrated that with a B/I protocol the ^{11}C-ABP688 distribution in late scans reflects the pattern of the total distribution volume and is therefore a measure for the density pattern of mGluR5. The early scans following injection are related to blood flow, although not in a fully quantitative manner. The advantage of the B/I protocol is that no arterial blood sampling is required, which is advantageous in clinical studies.

Keywords: ^{11}C-ABP688; Bolus/infusion protocol; mGluR5 receptor; PET; Ridge regression fitting

1. Introduction

Recently, ^{11}C-ABP688 (3-(6-methyl-pyridin-2-ylethynyl)-cyclohex-2-enone-*O*-^{11}C-methyl-oxime) has been introduced as a PET tracer to evaluate the metabotropic glutamate receptor mGluR5 [1]. This compound binds with high selectivity to the allosteric site of the receptor. In previous studies, we assessed the in vivo kinetics of ^{11}C-ABP688 after bolus injection and evaluated several quantification methods for human ^{11}C-ABP688 data. We demonstrated that ^{11}C-ABP688 has a high first-pass extraction fraction of 96%, that a two-tissue compartment model is required for adequately describing the tissue kinetics, that K_1 is highly correlated with regional cerebral blood flow and that there is an excellent agreement between the total distribution volumes calculated with the two-tissue compartment model and the Logan method [2].

Quantitative PET studies after bolus injection involve arterial blood sampling with complex blood analyses, which is inconvenient for patients. An alternative is the application of an equilibrium paradigm. If it is possible to reach true equilibrium, the concentration of total tracer in plasma equals that in tissue water, and the total tissue volume of distribution (Vt) equals the concentration of tracer in tissue divided by the concentration of authentic tracer in plasma [3]. For radiotracers with sufficient clearance such as ^{11}C-

* Corresponding author. Tel.: +41 44 255 4015; fax: +41 44 255 4428.
E-mail address: cyrill.burger@usz.ch (C. Burger).

0969-8051/$ – see front matter © 2010 Elsevier Inc. All rights reserved.
doi:10.1016/j.nucmedbio.2010.04.107

ABP688, the constant infusion of tracer will result in a prolonged state of equilibrium at the receptor population of interest [4]. To minimize the time to equilibrium, the infusion can be optimized by the addition of an initial bolus [3]. The optimal relation between bolus activity and infusion rate in such bolus/infusion (B/I) experiments can be derived based on the tissue uptake curves from a bolus-only experiment [3]. In practice, this relation is determined from the data of a series of bolus studies and then applied for the B/I studies. Treyer et al. [2] used the parameters resulting from fitting the two-tissue compartment model for the determination of a bolus/infusion ratio. A value of K_{bol}=53 min was found, meaning that a bolus equivalent to an infusion of 53 min should result in an equilibrium after about 40 min. In addition, the tracer accumulation shortly after injection of the bolus part can potentially be used as a measure for perfusion [5]. Often, fully quantitative studies are too noisy or the study population is too small to demonstrate significant differences. In these circumstances, the noise can be reduced by normalization of the regional tracer uptake to a specific region. The purpose of this study was to test the hypothesis that the pattern of the ^{11}C-ABP688 uptake using the B/I protocol corresponds to the total distribution volume at a later time point and to the perfusion at early time points. For this purpose, the tracer uptake at early and late time points was normalized to the mean of gray matter, cerebellum and white matter, and the values were compared to the corresponding ones obtained by tracer kinetic modelling of the ^{11}C-ABP688 kinetics after bolus only injection.

2. Materials and methods

2.1. Study population

Five healthy male volunteers (mean age 32 years; range 24–46 years) were scanned with both the bolus and the B/I protocol. The bolus study was performed first, and the time interval to the infusion study ranged from 7 to 97 days (mean 30 days). A detailed questionnaire was used to ensure that none of the volunteers had a history of neurologic disorders, drug or alcohol abuse, or psychiatric medication. The study was approved by the local ethics committee, and written consent was obtained from each volunteer.

2.2. PET Acquisitions

The PET acquisitions were performed using two similar whole-body PET-CT scanners (Discovery STE and Discovery RX, GE Healthcare, Milwaukee, WI, USA). The Discovery RX was only used for a single acquisition and the Discovery STE for all others. The volunteers were prepared with an antecubital vein catheter for tracer injection, and for the bolus studies also with a contralateral radial artery catheter for blood sampling. The acquisition was started with a low-dose CT for attenuation correction purposes, followed by the dynamic 3D PET acquisition (10×1 min, 10×5 min) which was started at tracer injection. In the bolus study, a slow bolus injection of 600–650 MBq ^{11}C-ABP688 PET within 2 min was applied. In the B/I study, the same activity was prepared in a syringe. It was applied using an initial 47-s bolus (48% of activity, infusion rate 30 ml/min), followed by a 1-h infusion (0.45 ml/min) of the remaining activity using a Perfusor fm (Braun) pump. With this B/I protocol, the activity injected by the bolus equals the activity infused by 53 min of infusion (disregarding physical decay). Transaxial images of the brain were reconstructed using the 3D FORE FBP algorithm with CT-based attenuation correction. The resulting images had a 128×128 matrix, 47 slices, 2.34×2.34×3.27-mm voxels and an in-plane resolution of approximately 7 mm. For measuring the arterial input curve of the bolus studies, arterial blood samples were collected every 30 s during the first 6 min, and then at increasing intervals until the end of the study. In the B/I studies, only two venous blood samples were collected at 60 min. The activity concentrations of whole blood and of authentic tracer in plasma were determined with the methods established by Treyer et al. [2].

2.3. Data analysis

2.3.1. Data processing of bolus studies

Motion correction was first applied to the images of the bolus studies. The average of Frames 2 to 4 was used as the reference, to which all frames were matched using the normalized mutual information criterion [6]. Parametric maps of the bolus studies were generated by fitting a standard two-tissue compartment model including a fixed 5% fraction of whole-blood activity with fit parameters K_1, K_1/k_2, k_3, k_4 to the voxel-wise time–activity curves (TACs). Because of the noise level, a ridge-regression fitting approach was applied as described in Appendix A. The voxel-wise fits resulted in parametric maps of all model parameters. The Logan plot was applied to the voxel-wise TACs for calculating reliable parametric maps of Vt (Vt_{Logan}) [2]. For the quantitative comparison, regional Vt and K_1 values were calculated by averaging the parametric maps within the VOIs. The PMOD version 3.0 software (PMOD Technologies, Zurich, Switzerland) was used for all image processing and quantification steps.

2.3.2. Data processing of infusion studies

No input curve was available for the infusion studies. The tracer accumulation was averaged over the last three frames (45-60 min, A_{late}) to obtain the late uptake pattern and over the first three frames (1–3 min, A_{early}) for the early uptake. The maps of A_{late} and A_{early} were rigidly matched to the corresponding bolus study maps using the Vt maps and an automatic registration method based on the normalized mutual information criterion [6]. VOI averages were calculated in the realigned parametric maps using the VOIs described below.

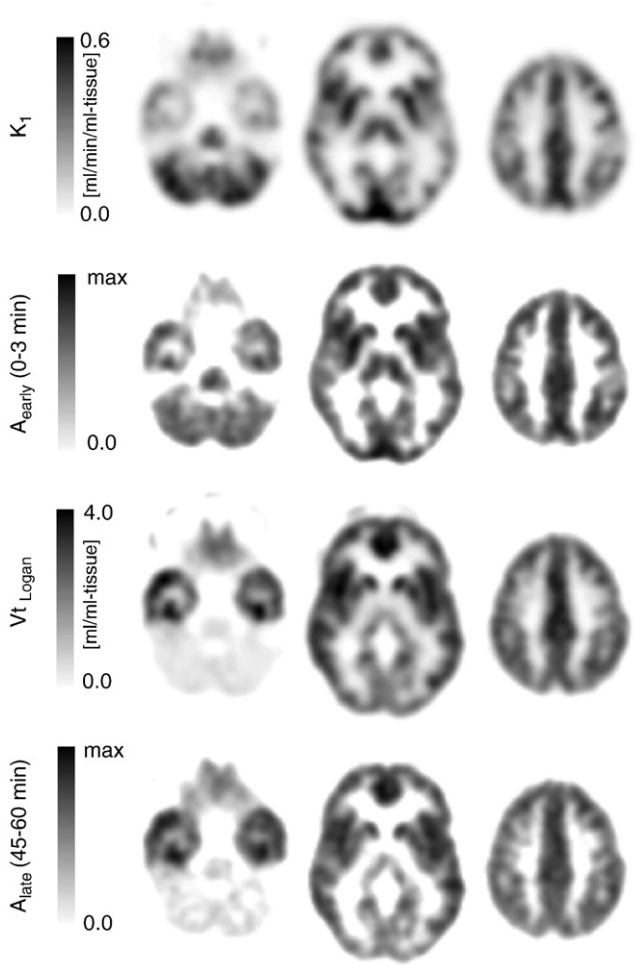

Fig. 1. Representative parametric maps calculated from a bolus study (K_1, Vt_{Logan}) and the corresponding B/I study (average activity 0–3 min and uptake 45–60 min). Note the marked difference between the early and late scans. In the late B/I scans, structures with low concentrations of mGluR5, such as the brain stem, thalamus and cerebellum, demonstrate a low tracer uptake and the pattern correlates well with the Vt_{Logan} maps. In the early scans, the pattern of tracer uptake agrees well with the K_1 maps.

2.3.3. Volume-of-interest definition

The VOI analysis was based on the standard VOIs defined by the AAL template [7]. To avoid spatially normalizing the PET images, AAL VOIs adjusted for each patient were obtained by the following approach: the K_1 map of the bolus study was spatially normalized to the standard MNI PET template. The resulting normalized K_1 image was then again normalized, this time using the original K_1 image as the reference. The resulting transformation constitutes an inverse normalization from the standard MNI space to the subject space. This transformation was applied to the AAL VOI template, resulting in the 113 standard AAL VOIs adjusted to the subject's anatomy. A subset of these VOIs were combined to form 13 standard VOIs: four cortical VOIs (frontal, parietal, temporal and occipital), two VOIs within the cingulate gyrus (anterior and posterior), three VOIs in the prosencephalon (caudate, putamen and thalamus), three VOIs in the limbic systems (medial orbitofrontal cortex, amygdala, hippocampus) and one VOI in the cerebellar cortex.

2.3.4. Parameter value normalization and bolus to B/I comparison

For facilitating the comparison between the different protocols, parameter normalization was performed using the average parameter values in gray matter, white matter and cerebellum. The gray matter and cerebellum values were obtained by applying AAL-VOIs, whereas individually defined VOIs were used for obtaining the white matter values. The normalized parameter values were compared by correlation and Bland–Altman analysis.

3. Results

Representative maps of the different parameters of interest are shown in Fig. 1. The similarity of K_1 and the early uptake A_{early} is evident, as well as the similarity of

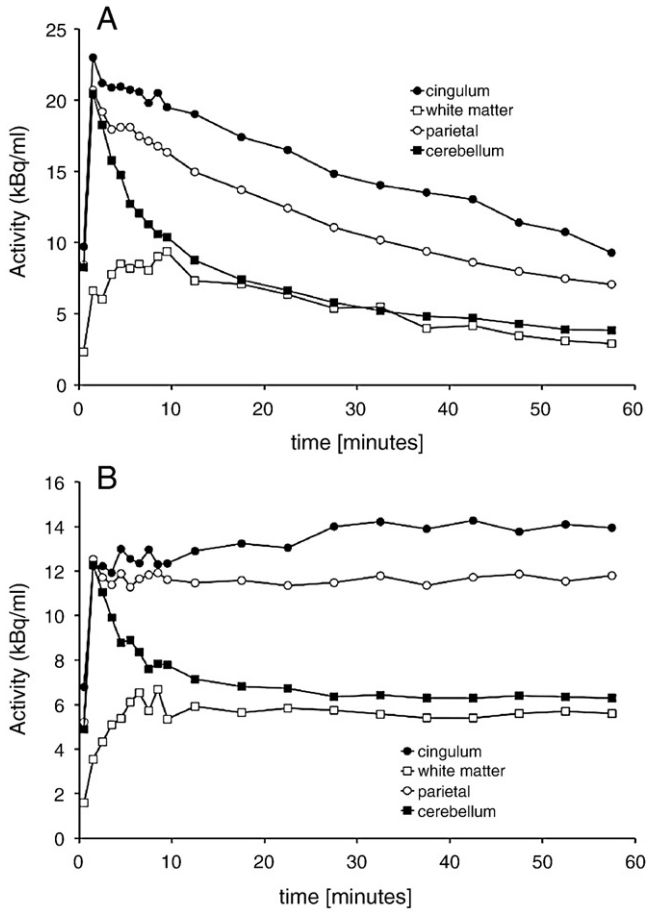

Fig. 2. Representative time–activity curves of a bolus study (A) and the corresponding B/I study (B). The values represent the mean in a volume of interest placed over the cingulate, parietal cortex, cerebellum and white matter. To facilitate a comparison, the gray matter curves were normalized to the cerebellum uptake in the second frame, namely, 22.3 kBq/ml in the bolus and 11.4 kBq/ml in the B/I study.

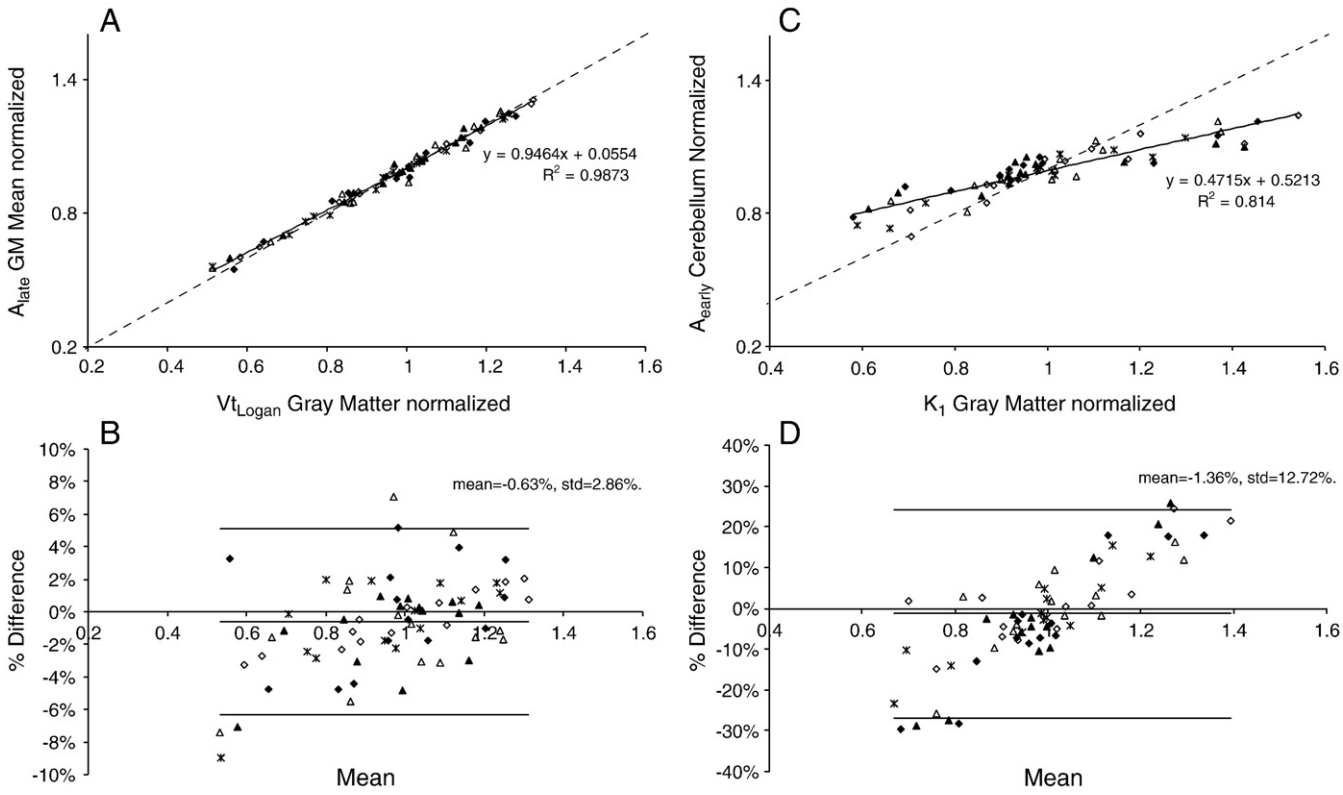

Fig. 3. (A) Scatter plot of 65 normalized values from five paired ^{11}C-ABP688 bolus and B/I studies. The Vt values were calculated as the VOI averages of the Vt_{Logan} maps (horizontal axis, bolus studies) and as the VOI average of the uptake from 45 to 60 min (A_{late}, vertical axis, B/I studies). Normalization was done relative to the average in all gray matter VOIs. (B) Bland–Altman plot showing the percent differences vs. the averages of the normalized Vt_{Logan} and A_{late} values. (C) Scatter plot of the perfusion-related information. The K_1 values were calculated as the VOI averages of the K_1 maps (horizontal axis, bolus studies) and as the VOI averages of the uptake during the first 3 min (A_{early}, vertical axis, B/I studies). Normalization was done relative to the average in all gray matter VOIs. (D) Bland–Altman plot showing the percent differences vs. the averages of the normalized K_1 and A_{early} values.

Vt_{Logan} and the late uptake A_{late}. The most visually appreciated difference between early and late uptake is in the cerebellum, the thalamus and the brain stem, where the initial uptake shows larger values.

Typical tissue TACs of the bolus and the B/I protocol are demonstrated in Fig. 2. In the cingulum and the cerebellum, a plateau is reached after 35 min; in the parietal cortex and white matter, it was already reached earlier. In addition, the early phase in white matter is protracted, due to the lower blood flow.

The comparison of Vt_{Logan} with the differently normalized A_{late} values is shown in Figs. 3–5A and B. The scatter plot demonstrates a high linear correlation close to the identity line between the normalized Vt estimates and A_{late} for all normalization methods. The highest correlation coefficient was calculated for the normalization to gray matter, the lowest for the normalization to white matter. In the Bland–Altman plots, only a few data points were outside the range mean±2 S.D. A somewhat different picture arises for the normalized early scans as demonstrated in Figs. 3–5C and D. The correlation of A_{early} with K_1 is reasonable for the normalization to gray matter and cerebellum but low for the normalization to white matter. A considerable intercept for all modes of normalization is notable. Furthermore, a flow-dependent trend is clearly seen in the Bland–Altman plots.

4. Discussion

This study validates the hypothesis that the pattern of the late distribution of ^{11}C-ABP688 with a B/I protocol reflects the pattern of the total distribution volume of the tracer and that the early distribution is related to K_1 and therefore blood flow. In this study, we concentrated on the pattern (normalized values) as opposed to absolute Vt values, since these can be obtained without arterial blood sampling, which renders the B/I protocol more practical. The reasons for testing three different regions as a normalization reference were the following. To demonstrate regional differences in the pattern of tracer uptake between groups, one often uses statistical parametric mapping, which was originally developed for blood flow activation studies. Most of these studies require some kind of normalized values, and the most common area of normalization is the gray matter. This normalization method yielded the highest correlation of the late uptake pattern with the Vt values and also at early time points with K_1. A disadvantage of this normalization is that the gray matter in the hemispheres also contains the mGluR5 receptors. Therefore, a general increase or decrease of mGluR5 would be missed by this method. However, localized differences in the mGluR5

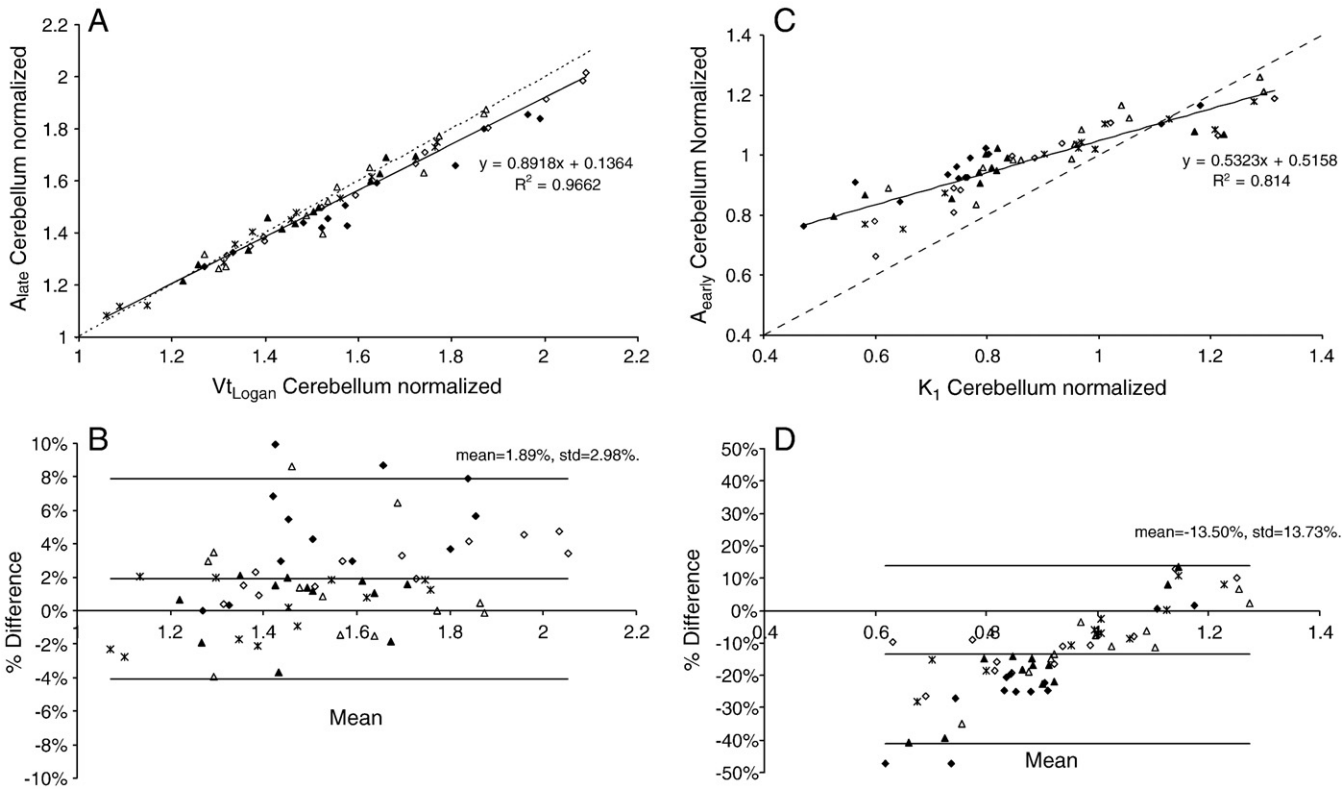

Fig. 4. Similar plots as in Fig. 3 except that normalization was performed relative to the average in the cerebellum VOI.

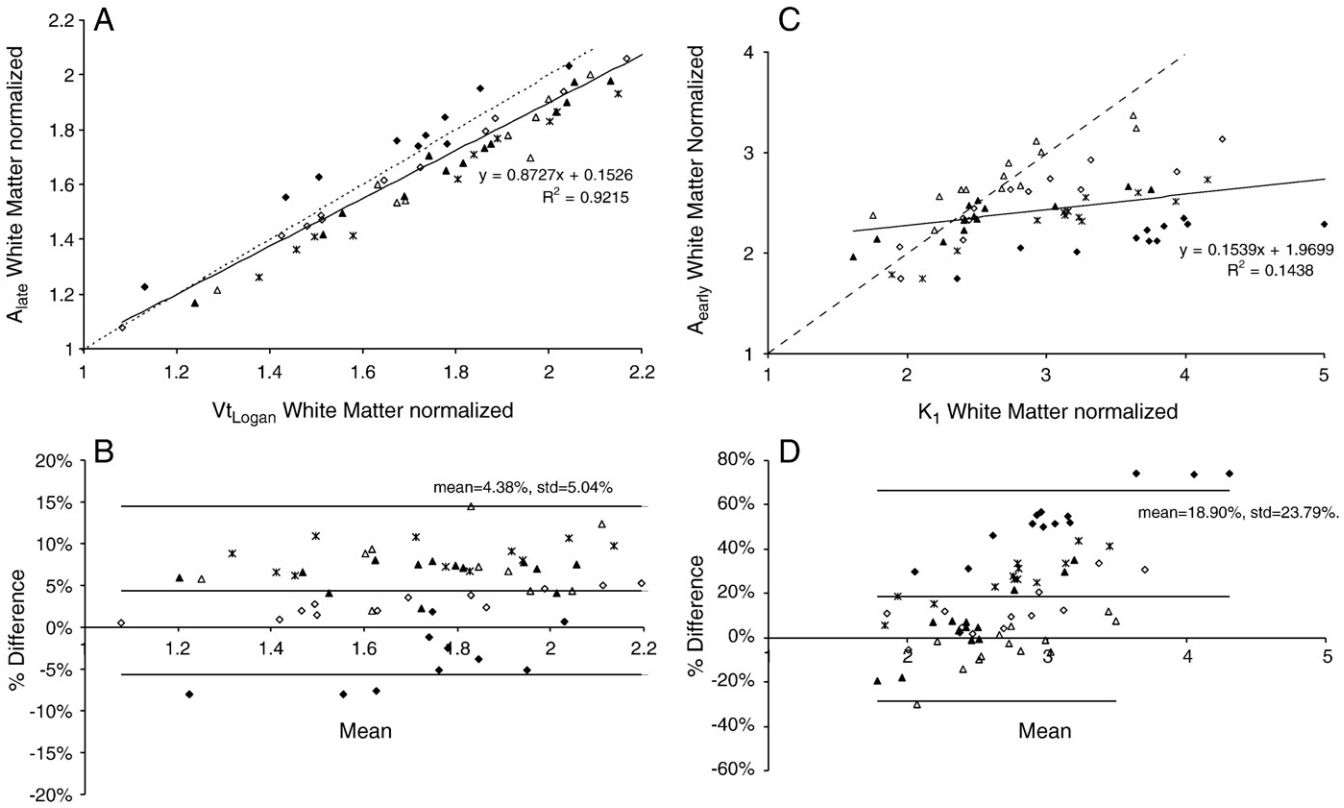

Fig. 5. Similar plots as in Fig. 3 except that normalization was performed relative to the average in the white matter VOI.

distribution could still be demonstrated. In certain cases, it would be advantageous to normalize the tissue uptake to an area with few, or ideally no, mGluR5. The gray matter area with the lowest concentration of mGluR5 is the cerebellum. In the rat cerebellum, there is no measurable concentration of mGluR5 [1]; in humans, the cerebellar mGluR5 concentration is low but probably not negligible [8]. The maps normalized to the cerebellum also demonstrate a high correlation with the normalized Vt and K_1 maps, although the noise is somewhat higher compared to the normalization to gray matter.

The area with negligible mGluR5 in humans is the white matter. The advantage of this normalization is that it potentially allows to partially quantify differences in mGluR5 concentration between groups. If one assumes that the nonspecific ^{11}C-ABP688 uptake in white matter is equal in both groups, any percentage change in the normalized values between the groups will reflect the same percentage change in Vt. However, the normalization to white matter yielded the correlation with the highest noise. While the normalized late scans still correlate reasonably well with normalized Vt, the correlation of the early scans with the K_1 maps is poor.

The delivery of tracer by tissue perfusion is a critical step of tracer uptake. Due to the high correlation of K_1 with regional cerebral blood flow, which is a consequence of the high first-pass extraction fraction of ABP688 [2], K_1 can be used as a measure of perfusion in absolute units. Consequently, parametric maps of K_1 represent supplemental information which may be valuable for the interpretation of the total distribution volume outcome. The K_1 maps were calculated using a two-tissue compartment model with ridge regression fitting. As the K_1 parameter is directly proportional to the calculated model function, it can relatively reliably be estimated, as has been found by Zhou et al. [9]. Averaging the first minutes of tracer uptake yields an image which can be expected to be related to tracer delivery, but which is not an absolute perfusion measure. The correlations of the early uptake with the K_1 maps deviate considerably from the identity line. Lower blood flows are relatively overestimated and high blood flows relatively underestimated. The reason for this effect is the backdiffusion of tracer to blood during the integration time. The higher the blood flow (K_1) and the longer the integration time, the higher the amount of backdiffused tracer. The correlation could therefore be improved by shortening the integration time, but that would lead to noisier images. We found that 3 min was a reasonable compromise.

The uptake at late time points will exactly reflect Vt if the tracer concentration in tissue and blood were in true equilibrium. That this is indeed the case is suggested by the plateau in tissue activity which is reached in the B/I studies. However, a proof of a true equilibrium would require the demonstration of a steady concentration of true tracer also in arterial plasma. In true equilibrium, absolute values for Vt using the B/I protocol could be derived by dividing the tissue activity values by the activity values in arterial plasma. In fact, it might be possible to measure blood concentration in venous plasma, since at late time points, arterial and venous values converge.

5. Conclusion

It is demonstrated that, with a B/I protocol, the ^{11}C-ABP688 distribution in late scans reflects the pattern of the total distribution volume and is therefore a measure for the density pattern of mGluR5. The early scans following injection are related to blood flow, although not in a fully quantitative manner. The advantage of the B/I protocol is that no arterial blood sampling is required, which is advantageous in clinical studies.

Acknowledgment

The study was supported by the Swiss National Science Foundation (Grants 3100A0-105804/1 and PP00B-110751/1), OPO-Stiftung Zürich, the Novartis Institutes for BioMedical Research and the Zurich Center for Integrative Human Physiology (ZIHP).

Appendix A

To calculate the parametric maps of K_1, a standard two-tissue compartment model including a fixed 5% fraction of whole-blood activity was fitted using a ridge-regression approach. Ridge-regression fitting imposes a penalty on changing the individual model parameters from their respective starting values. Less identifiable parameters are subject to a stronger penalty.

K-Means clustering and parameter starting values

The starting values were automatically determined by the following approach: background voxels were removed by calculating the signal energy of the voxel-wise TACs (sum of squared TAC values) and masking all voxels below 0.1% of the maximal energy. The remaining voxels were classified into 10 clusters using a *k*-means algorithm [10]. The time-weighted Euclidean distance was used as the measure of dissimilarity between TACs. Ten voxels serving as initial cluster centroids were randomly assigned. In a first step, each voxel was assigned to the centroid with minimal distance, thus forming 10 initial clusters. For each cluster, a centroid TAC was calculated as the average TAC of all voxels in the cluster. Subsequently, an iterative process was started which repeated the following two steps: (1) Each voxel TAC was compared with all centroid TACs and assigned to the cluster with minimal distance. (2) All centroid TACs were recalculated to reflect the updated cluster population. The iterations were repeated until no voxel was reassigned to a different cluster, or the number

of 300 iterations was exhausted. The final centroid TACs were fitted by a standard two-tissue compartment model including a fixed 5% fraction of whole-blood activity, yielding 10 sets of fit parameters (K_1, K_1/k_2, k_3, k_4) together with estimates of their standard errors derived from the fitting covariance matrix of the Marquardt–Levenberg algorithm.

Nonlinear ridge-regression fitting

For the iterative nonlinear fitting of the voxel-wise TACs with a two-tissue compartment model, the standard cost function "weighted residuals sum of squares" (WRSS) was extended by a term which penalizes the local parameter variation [11,12]. This total sum of squares (TSS) criterion is given by the expression [9]

$$\mathrm{TSS}(\theta) = \mathrm{WRSS}(\theta) + \sum_{i=1}^{p} h_i(\theta_i - \beta_i)^2$$

where θ denotes the parameter set to be optimized, β_i the initial parameter estimates and h_i the ridge factors for the p fitted parameters. This TSS criterion was integrated into the Marquardt–Levenberg optimization, including the calculation of the Hessian and gradient matrices.

For performing the voxel-wise ridge-regression fits, for each parameter a β_i image is needed which provides a reasonable approximation of the final parameter value. Assuming successful clustering and stable fits of the centroid TACs, β_i images were obtained by creating cluster images using the parameter values resulting from the centroid TAC fits and by applying a spatial filter to accommodate smooth transitions. A simple average filter was used which replaced a voxel value by the average of a 5×5×3 neighbourhood (5×5 voxels in-plane, three voxels axially).

The ridge factors h_i should be chosen such that changes of unstable parameters are penalized to a stronger extent. Assuming that a large standard error (ste) indicates a parameter which suffers from a high variability, it was included in the ridge factors [11]. To allow more variation for parameters with a large value range across the clusters, the ridge factors were finally calculated by

$$h_i = \left(\frac{\mathrm{median}(\mathrm{ste}_i)}{\mathrm{median}(\beta_i)\,\mathrm{range}(\beta_i)} \right)^2$$

Median(x_i) represents the median of the parameter x_i across the 10 cluster fits, and range(β_i) the absolute difference between the maximal and the minimal fit value. The ridge factors were smoothed in the same way as the initial parameters. Additionally, the user interface supports a scaling factor for each h_i value to allow for manual adjustments of the individual parameter penalties. This scaling was set to a factor of 100 for all h_i.

References

[1] Wyss MT, Ametamey SM, Treyer V, Bettio A, Blagoev M, Kessler LJ, et al. Quantitative evaluation of (11)C-ABP688 as PET ligand for the measurement of the metabotropic glutamate receptor subtype 5 using autoradiographic studies and a beta-scintillator. Neuroimage 2007;35:1086–92.

[2] Treyer V, Streffer J, Wyss MT, Bettio A, Ametamey SM, Fischer U, et al. Evaluation of the metabotropic glutamate receptor subtype 5 using PET and ^{11}C-ABP688: assessment of methods. J Nucl Med 2007;48:1207–15.

[3] Carson RE, Channing MA, Blasberg RG, Dunn BB, Cohen RM, Rice KC, et al. Comparison of bolus and infusion methods for receptor quantitation: application to [^{18}F]cyclofoxy and positron emission tomography. J Cereb Blood Flow Metab 1993;13:24–42.

[4] Bressan RA, Erlandsson K, Mulligan RS, Gunn RN, Cunningham VJ, Owens J, et al. A bolus/infusion paradigm for the novel NMDA receptor SPET tracer [^{123}I]CNS 1261. Nucl Med Biol 2004;31:155–64.

[5] Koeppe RA, Gilman S, Joshi A, Liu S, Little R, Junck L, et al. ^{11}C-DTBZ and ^{18}F-FDG PET measures in differentiating dementias. J Nucl Med 2005;46:936–44.

[6] Studholme C, Hill D, Hawkes D. An overlap invariant entropy measure of 3D medical image alignment. Pattern Recognition 1999;46:936–44.

[7] Tzourio-Mazoyer N, Landeau B, Papathanassiou D, Crivello F, Etard O, Delcroix N, et al. Automated anatomical labeling of activations in SPM using a macroscopic anatomical parcellation of the MNI MRI single-subject brain. Neuroimage 2002;15:273–89.

[8] Ametamey SM, Treyer V, Streffer J, Wyss MT, Schmidt M, Blagoev M, et al. Human PET studies of metabotropic glutamate receptor subtype 5 with ^{11}C-ABP688. J Nucl Med 2007;48:247–52.

[9] Zhou Y, Huang SC, Bergsneider M, Wong DF. Improved parametric image generation using spatial-temporal analysis of dynamic PET studies. Neuroimage 2002;15:697–707.

[10] Velamuru PK, Renaut RA, Guo H, Chen K. Robust Clustering of Positron Emission Tomography Data. Joint Conference of the Classification Society of North America and Interface Foundation of North America, St. Louis; 2005.

[11] Byrtek M, O'Sullivan F, Muzi M, Spence M. Use of ridge regression for improved estimation of kinetic constants from PET data. IEEE Trans Nuclear Science 2005;52:63–8.

[12] O'Sullivan F, Saha A. Use of ridge regression for improved estimation of kinetic constants from PET data. IEEE Trans Med Imaging 1999;18:115–25.